Memory-function approach to interacting quasiparticle-boson systems

V. M. Kenkre and S. Raghavan
Center for Advanced Studies and Department of Physics and Astronomy, University of New Mexico, Albuquerque, New Mexico 87131

A. R. Bishop and M. I. Salkola
Theoretical Division, Los Alamos National Laboratory, Los Alamos, New Mexico 87545

(Received 7 July 1995)

The fundamental problem of the effects of strong interactions with lattice vibrations on quasiparticle transport is analyzed with the help of the memory-function approach introduced many years ago in the context of exciton and charge transport in molecular aggregates. Comparison is made among the exact evolution in a simplified system, the predictions of the memory approach, and evolution based on semiclassical arguments. It is shown that, for a number of physically relevant parameter ranges, the memory approach provides an excellent representation of the exact evolution while the semiclassical approach does not. A quantum yield experiment appropriate to sensitized luminescence is examined in the light of the exact evolution and the various approximations. Three physical systems are also discussed. They involve charge transport in aromatic hydrocarbon crystals, thermal conduction in refractory materials, and vibrational energy transfer in biological systems.

I. INTRODUCTION

Strong electron-phonon interactions constitute one of the central areas in condensed-matter physics. Many basic aspects of the effects of these interactions on quasiparticle dynamics are not understood despite much work that has been carried out. The effects are of interest in such widely different fields as charge transport in narrow-band materials,[1–3] Frenkel exciton transport in molecular crystals,[4–6] hydrogen diffusion in metals,[7] and muon spin relaxation.[8] Various theoretical approaches have been developed. They involve polaron concepts,[1,3,9] stochastic methods,[5,10] dressing transformations,[1,3,4,11,12] and, more recently, semiclassical methods and the discrete nonlinear Schrödinger equation.[13–17] The latter two have come under criticism in the light of careful studies[18–20] of their range of validity, and the question has been raised whether they are real consequences of quantum mechanics or merely artifacts of approximation schemes.[18] Recent work by the present authors[22] has shown that, while the semiclassical approximation can be often inaccurate as has been shown in Refs. 18–21, it is an exact consequence of the quantum evolution in a clearly defined limit. The work has also shown that the memory-function approach developed earlier in the context of exciton and charge transport[6,11,12] can be remarkably accurate in dealing with quasiparticle transport in systems for whose description the semiclassical approximation and the discrete nonlinear Schrödinger equation have been used recently. This second finding has motivated the study to be reported here. The purpose of the present paper is to reintroduce the memory-function approach in the modern context, and to discuss physical issues of quasiparticle transport within its framework.

The paper is set out as follows. The essence of the memory-function approach, the agreement its predictions show with numerically obtained solutions of arbitrary accuracy, and a physical understanding of quasiparticle evolution in its terms form Sec. II. Two other approximation methods are discussed in comparison to the memory approach in Sec. III. An application of the memory approach to observations of the quantum yield is made in Sec. IV, parameters of the memory functions in three experimental systems are discussed in Sec. V, and concluding remarks form Sec. VI.

II. MEMORY-FUNCTION APPROACH

The system of interest is a quasiparticle moving among the sites of a lattice (crystal or molecular aggregate) while interacting strongly with the vibrations of a lattice. Specifically, the Hamiltonian is

$$\hat{H}=\sum_m \epsilon_m a_m^\dagger a_m+\sum_{m,n} V_{mn}a_m^\dagger a_n+\sum_q \hbar\omega_q\left(b_q^\dagger b_q+\frac{1}{2}\right)$$
$$+N^{-1/2}\sum_{m,q}\hbar\omega_q g_q \exp(i\mathbf{q}\cdot\mathbf{R}_m)(b_q+b_{-q}^\dagger)a_m^\dagger a_m . \tag{2.1}$$

Here $a_m^\dagger$ creates a quasiparticle with energy ϵ_m at site m in a system of N sites, $b_q^\dagger$ creates a phonon with wave vector q and frequency ω_q, V_{mn} is the intersite matrix element between sites m and n, and g_q is the dimensionless quasiparticle-phonon coupling constant. The quantities $\mathbf{q}$ and $\mathbf{R}_m$ are vectors in the reciprocal and direct lattices, respectively, $\mathbf{R}_m$ being the lattice vector which locates site m. For the sake of simplicity, we restrict our analysis in the present paper to a quasiparticle moving between the sites of a degenerate two-site system (a dimer) with interaction matrix element V, while being in strong interaction with a single vibrational mode of frequency ω with coupling constant g. The Hamiltonian of (2.1) simplifies, for this system, to[23]

$$\hat{H}=V\hat{r}+g\omega\hat{y}\hat{p}+\frac{1}{2}\omega(\hat{y}^2+\hat{\pi}_y^2), \tag{2.2}$$

where the quasiparticle operators $\hat{p},\hat{q},\hat{r}$ are defined as $\hat{p}=a_1^\dagger a_1-a_2^\dagger a_2$, $\hat{q}=-i(a_1^\dagger a_2-a_2^\dagger a_1)$, and $\hat{r}=a_1^\dagger a_2+a_2^\dagger a_1$. The operators $\hat{y}$ and $\hat{\pi}_y$, obey the commutation relation $[\hat{y},\hat{\pi}_y]=i$ and describe a harmonic oscillator of frequency ω. Here and henceforth, $\hbar$ has been set equal to 1.

The memory-function approach to dynamics was developed[6,11,12] to address quasiparticle transport in the regime of strong coupling with vibrations. While memory functions and the relevant analysis have also been given[6,12] for spatially extended systems, we will present the details here only for the two-site dimer of (2.2). The well-known transformation[1,11,24,25] defined by the prescription,

$$\hat{A}=\exp(-ig\hat{\pi}_y\hat{p})\hat{a}\ \exp(ig\hat{\pi}_y\hat{p}), \tag{2.3}$$

where, corresponding to any operator $\hat{a}$, the transformed operator is $\hat{A}$, leads to

$$\hat{p}=\hat{P}, \tag{2.4}$$

$$\hat{q}=\hat{Q}\ \cos(2g\hat{\Pi}_Y)-\hat{R}\ \sin(2g\hat{\Pi}_Y), \tag{2.5}$$

$$\hat{r}=\hat{Q}\ \sin(2g\hat{\Pi}_Y)+\hat{R}\ \cos(2g\hat{\Pi}_Y), \tag{2.6}$$

$$\hat{y}=\hat{Y}-g\hat{P}, \tag{2.7}$$

$$\hat{\pi}_y=\hat{\Pi}_Y. \tag{2.8}$$

In terms of these transformed operators, the Hamiltonian can be expressed as

$$\hat{H}=V[\hat{R}\ \cos(2g\hat{\Pi}_Y)+\hat{Q}\ \sin(2g\hat{\Pi}_Y)]+\frac{\omega}{2}\ (\hat{Y}^2+\hat{\Pi}_Y^2) -\frac{g^2\omega}{2}\ \hat{1} \tag{2.9}$$

with the help of the fact that $\hat{P}^2$ equals the identity operator $\hat{1}$.[26] The application of projection operators[12,27] that diagonalize in the site representation of the quasiparticle and trace over the phonons, leads to the following equation of evolution for the probability difference $p(t)$:

$$\frac{dp(t)}{dt}+2\int_0^t ds\ \mathscr{W}(t-s)p(s)=\mathscr{I}(t). \tag{2.10}$$

Equation (2.10) involves no approximations. Flexibility in the choice of projection operators[28] allows one to make $\mathscr{I}(t)=0$ identically provided the initial state of the system is diagonal in the site representation of quasiparticle and an outer product of quasiparticle and vibrational states. With the help of a perturbation expansion in the transfer, specifically in the first of the three terms of (2.9), an approximate expression for the memory function $\mathscr{W}(t)$ is then obtained. For an initial vibrational condition that is thermal in the transformed oscillator states, one obtains

$$\mathscr{W}(t)=2V^2\ \mathrm{Re}(e^{h(t)-h(0)}). \tag{2.11}$$

The result for $h(t)$ in (2.11), valid for the case when the number of vibrational modes is arbitrary rather than 1 as in (2.2), is[11]

$$h(t)=2\sum_q\ g_q^2[\exp(-i\omega_q t)+2n_q\ \cos(\omega_q t)]. \tag{2.12}$$

The effects of temperature T are reflected in the Bose occupation numbers $n_q=[\exp(\beta\omega_q)-1]^{-1}$, with $\beta=1/k_BT$. At $T=0$, and if there is only one mode of vibration, (2.12) reduces to

$$h(t)=2g^2\ \exp(-i\omega t). \tag{2.13}$$

For the simple zero-T, single-mode dimer studied in this paper, the point of departure of the memory-function approach is thus the evolution equation

$$\frac{dp}{dt}+4V^2\int_0^t ds e^{-2g^2[1-\cos\ \omega(t-s)]}\cos[2g^2\ \sin\ \omega(t-s)]p(s)=0. \tag{2.14}$$

That this memory approach can give a rather accurate description of the evolution can be seen through a comparison (see Fig. 1) of exact calculations of $p(t)$ obtained numerically.[19,22] The exact calculational procedure consists of the numerical diagonalization of the Hamiltonian $\hat{H}$ in (2.2) expressed as a finite-dimensional matrix whose size is increased until convergence to any desired accuracy is obtained in the results. The parameter values are $g=3$, $\omega=2V$ in Fig. 1(a) and $g=1$, $\omega=15V$ in Fig. 1(b). In both cases, the memory approach (solid line) approximates the exact evolution (dashed line) rather well. The characteristic features of the exact evolution as seen in (a) and (b) are rapid oscillations followed by ''silent runs'' and revivals, and an overall long-time oscillation representing tunneling from one site to the other. This oscillation signifies the obvious fact that self-trapping cannot occur except on short-time scales. All these features are reproduced by the memory approach. By contrast, the well-known semiclassical approximation (dotted line), which forms the foundation of a large body of recent literature, including Refs. 13–17, fails on two counts: it predicts true self-trapping and is thus markedly different from the exact evolution on the long-time scale as is clear in (b), and it is unable to reproduce the characteristic silent runs [evolution with little change of $p(t)$] in between the rapid oscillation regions observed on the short-time scale as seen in (a), the semiclassical prediction being a structureless oscillation.[18–20,22]

Although the memory approach is obviously not exact, we have seen in our studies of various parameter cases of physical interest that the approach is able to reproduce many of the essential features of the exact evolution. The extent of the quantitative agreement is dependent on the choice of parameters, as expected. We have also seen that the memory approach can be vastly superior to the semiclassical approach for realistic choices of parameters. This conclusion will be reinforced in Sec. V where we will examine charge, heat, and excitation transport in three physical systems.

The exact evolution exhibits a hierarchy of time scales.[22] It is easy to understand the origin of the hierarchy in terms of the memory function in (2.14) since four of the characteristic times in the hierarchy are simply linked to corresponding times in the memory function itself. For appropriate parameters, the probability evolution exhibits rapid oscillations on

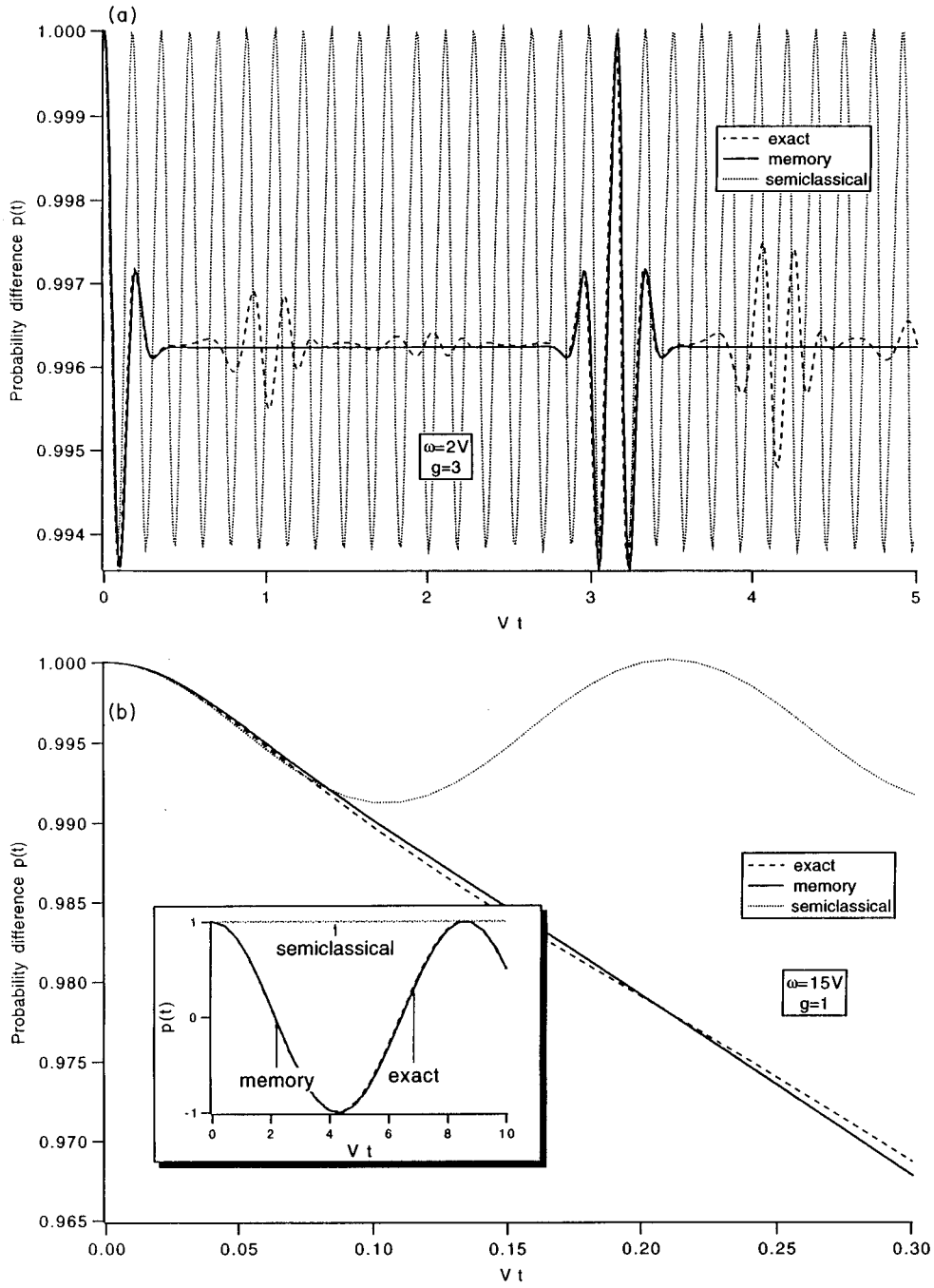

FIG. 1. Comparison of the predictions of (i) the memory-function approach (solid line), (ii) an exact numerical analysis of arbitrary accuracy (dashed line), and (iii) the standard semiclassical treatment (dotted line). Plotted is the probability difference p as a function of the dimensionless time Vt for two parameter sets: (a) $\omega=2V$, $g=3$, (b) $\omega=15V$, $g=1$. In (a), there is qualitative agreement among all three in that the self-trapping feature predicted by the semiclassical approximation is also shared, on the time scale shown, by the exact evolution and the memory approach. In (b), excellent agreement is obtained between the memory approach and the exact evolution, both of which show free motion represented by oscillations of p between 1 and -1, while the semiclassical approximation predicts self-trapping and is quite off the mark. Quantitatively, the semiclassical approximation is completely unable to reproduce the "silent runs" and related features of the exact evolution, while the memory function describes them adequately (but not completely). The inset in (b) describes long time evolution.

the time scale τ_χ, a decay on the scale τ_γ, a revival on the scale τ_Δ, and an overall oscillation on the scale τ_T. The first three of these times are immediately apparent in the time evolution of the memory itself, the fourth being related to the average value of the memory. The four time scales can be appreciated easily in the limit of small ω. The memory function in (2.14) then reduces to

$$\mathscr{W}(t)=2V^2e^{-g^2\omega^2t^2}\cos(2g^2\omega t). \tag{2.15}$$

The first factor of $\mathscr{W}(t)$ decays in a time characterized by the reciprocal of $g\omega$. Inside this decaying envelope, there are rapid oscillations whose period is characterized by the reciprocal of $g^2\omega$. The silent runs occur from the time the envelope decays to the time when the argument of the exponent in the first factor reaches near-zero values again, and possess a frequency ω. In this limit, it is thus possible to identify τ_χ, τ_γ, and τ_Δ with the reciprocals of $g^2\omega$, $g\omega$, and ω, respectively. It is also easy to see that the reciprocal of the tunneling time τ_T is simply related to the square root of the average value of $\mathscr{W}(t)$, i.e., to Ve^{-g^2}. Figure 2(a) shows the memory function (normalized to its initial value) for two parameter sets as shown. Figure 2(b) shows the consequence of the memory function on the probability evolution for one of the sets, viz., $\omega=3V$, $g=1.8$, along with the exact evolution. The various characteristics of the evolution, viz., the oscillation, the decay, the silent run and the revival, are clear from Fig. 2(a). The analytic form of the memory in (2.14) also makes transparent the source of the silent runs in $p(t)$.

The primary features of the exact evolution[19,22] are easily understood in terms of the evolution of a dimer whose inter-

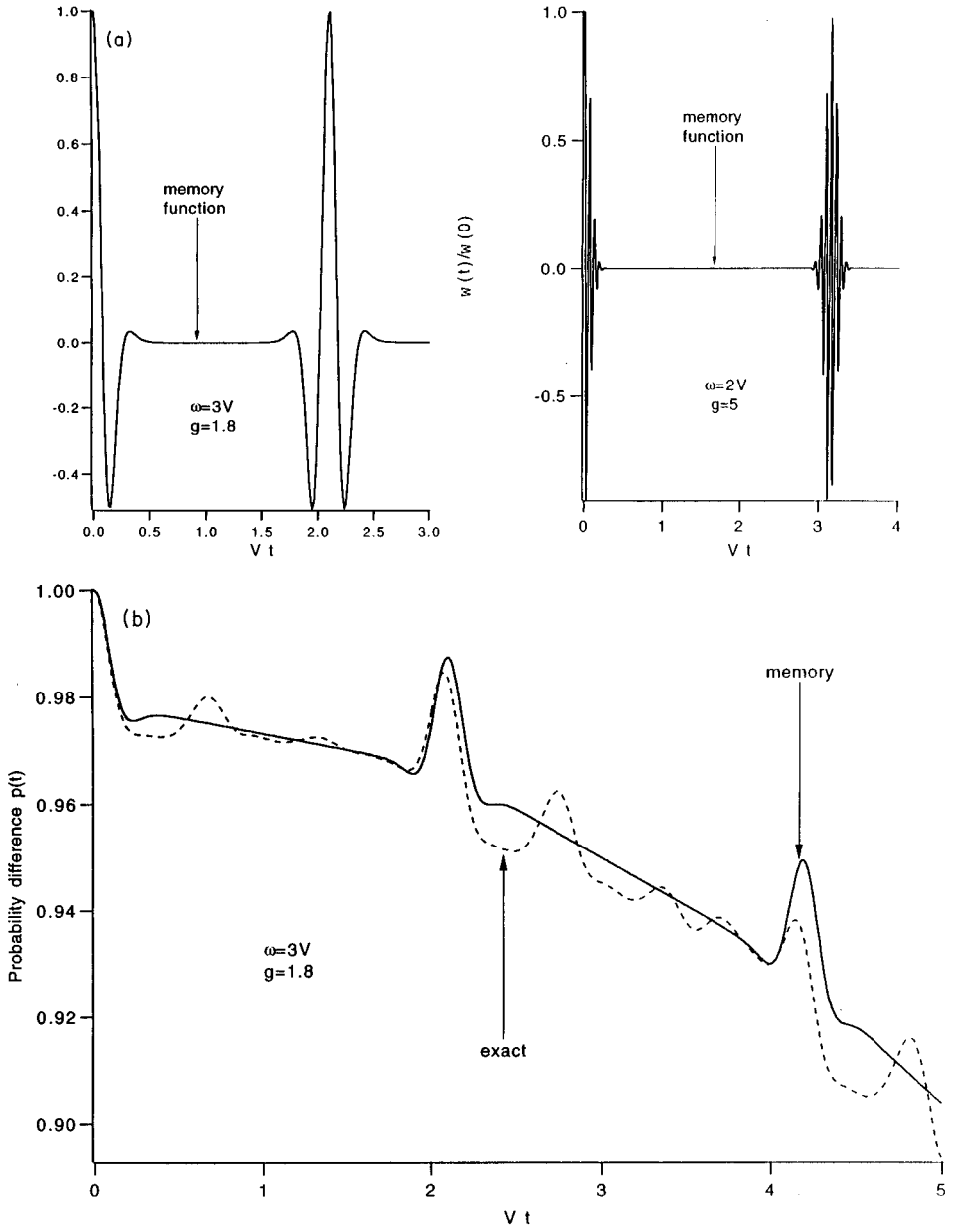

FIG. 2. Features of the memory function showing a hierarchy of time scales which are also reflected in the evolution of the probability difference. Shown in (a) are the memory functions. Parameters are $\omega=3V$, $g=1.8$ and $\omega=2V$, $g=5$. The high-frequency oscillations of the memory function are exhibited clearly for the latter case. Shown in (b) is evolution of the probability difference corresponding to the parameters $\omega=3V$, $g=1.8$.

action with the vibrations is represented entirely by a *time-dependent* energy mismatch $\chi(t)$ and intersite interaction $V(t)$. The semiclassical approximation (or the discrete nonlinear Schrödinger equation) captures the effects of $\chi(t)$ and is thus able to predict the transition from free to self-trapped behavior. However, it does not capture the $V(t)$ effect. During the vibrational oscillations, the overlap between the wave functions on the two sites repeatedly becomes near-vanishing (provided the coupling g is large enough). This interaction mismatch causes $V(t)$ to become effectively very small (bandwidth narrowing represented by Ve^{-g^2}). The absence of intersite interaction means that the motion of the quasiparticle is suppressed. This state of affairs persists for some time until the vibrational oscillation unmakes the mismatch. The wave function overlaps return to their original high values, and revival occurs. This happens repeatedly with period $2\pi/\omega$ and is the source of the silent runs. The success of the memory approach versus the semiclassical approximation lies in the presence of the effective time dependence of the intersite interaction in the memory approach.

III. COMPARISON TO SEMICLASSICAL APPROXIMATION SCHEMES

In this section, we compare the memory-function approach to two of the approximation schemes that have been put forward to describe the evolution governed by (2.1) or (2.2). Notable among such schemes are the semiclassical approximation and the discrete nonlinear Schrödinger equation. The relation of the latter to the former is well known.[13,14,16] We focus here only on the former which, for the dimer, is

$$\frac{dp}{dt}=-2Vq, \tag{3.1}$$

$$\frac{dq}{dt}=2Vp-2g\omega yr, \tag{3.2}$$

$$\frac{dr}{dt}=2g\omega yq, \tag{3.3}$$

$$\frac{dy}{dt}=\omega\pi_y, \tag{3.4}$$

$$\frac{d\pi_y}{dt}=-\omega y-g\omega\pi_y. \tag{3.5}$$

The absence of circumflexes over p,q,r,y,π_y means that the corresponding operators have been replaced here by their expectation values. This semiclassical approximation consists, as is well known, of replacing the expectation value of the products of operators by the product of expectation values of the operators. In addition to this *standard* semiclassical approximation, another classical approximation has appeared in the literature. Introduced by Brown, Lindenberg, and West[29] a few years ago as a better alternative to what they termed the Kenkre-Rahman memory function,[11] it replaces the complex quantity $h(t)$ by its classical counterpart. For the zero-T single-mode case this means that $2g^2\exp(-i\omega t)$ is replaced by $2g^2\cos(\omega t)$. Since this procedure employs a classical $h(t)$, we compare its consequences to the standard semiclassical results as well as to the predictions of our memory approach. We will refer to this approximation as the ''symmetrized'' memory approach because it involves the replacement of the autocorrelation function $\langle x(t)x\rangle$ of the oscillator displacement operator by the symmetrized classical counterpart $\langle x(t)x+xx(t)\rangle/2$. Such approximations are well-known in the classical limit of linear-response theory.[30] The evolution equation for the symmetrized memory approximation is[29]

$$\frac{dp}{dt}+4V^2\int_0^t ds\ e^{-2g^2[1-\cos\omega(t-s)]}p(s)=0. \tag{3.6}$$

Shown in Fig. 3(a) is a comparison between the memory-function result as given by (2.14), the numerically obtained exact result and the symmetrized approximation as given by (3.6). It is clear that, contrary to the suggestion in Ref. 29, the symmetrized approximation is not a better alternative to the memory approach. Instead, it fails significantly for the parameters shown. While the symmetrized memory does decay to a very small value in the same time as the Kenkre-Rahman memory, it lacks the key ingredient needed to produce the silent runs observed in the exact evolution for $p(t)$. As the direct result of the symmetrization procedure, the memory used in Ref. 29 lacks the second (cosine) factor, consequently does not oscillate, and does not give an integral that is approximately zero by the time the decay has occurred. The inset in Fig. 3(a) showing the comparison between the two memory functions should make this point quite clear. The fact that the time dependence of $h(t)$ is complex (rather than real) is a manifestation of the quantum-mechanical nature of the vibrations. Its neglect seriously distorts the probability evolution except at elevated temperatures where the Bose occupation factors considerably exceed 1. It is important to realize that, although the symmetrized approximation improves in its validity as the temperature increases, it *never* becomes preferable to (2.14), i.e., to the use of the original memory function of Refs. 6, 11, and 12.

In Fig. 3(b) we show the comparison of the memory approach to the standard semiclassical approach. The failure of the semiclassical approximation (3.5) for many parameter ranges, pointed out earlier by Grigolini and co-workers[18–20] is confirmed by our results. However, in the limit $g\to\infty,\omega\to 0,g^2\omega=$const, the semiclassical approximation approaches the exact result. Mathematically, this limit bears resemblance to the well-known $\lambda^2 t$ limit of van Hove.[31] Physically, it represents an infinitely massive oscillator.[22] This is clear from the fact that the interaction energy term $g\omega$ is proportional to the oscillator displacement which goes as $(\mu\omega)^{-1/2}$ while the phonon frequency ω is proportional to $\mu^{-1/2}$, μ being the oscillator mass. In this massive oscillator limit, $\mathscr{W}(t)$ takes on the simple form

$$\mathscr{W}(t)=2V^2\cos(\chi t) \tag{3.7}$$

the single time scale that survives is τ_χ, equivalently the reciprocal of $\chi=2g^2\omega$, and the tunneling time becomes infinite, giving true self-trapping. Whereas the validity of the standard semiclassical approximation improves in this massive oscillator limit, the symmetrized approximation of Ref. 29 improves as $g\to 0,\omega\to 0$, which merely signifies weak coupling. We have also analyzed semiclassical approximations other than the two analyzed above and will comment on them elsewhere.

IV. APPLICATION TO SENSITIZED LUMINESCENCE

We now apply the memory-function approach to a simple experiment that brings out the essential features of the dynamics of the problem. Let the quasiparticle moving between the sites of the dimer be an electronic excitation which decays radiatively. Assume that a trap extracts the excitation from one of the sites. The trap probability may be monitored by measuring the quantum yield, i.e., the ratio of the number of photons emitted (radiatively) by the trap to the number of electronic excitations put initially into the system. This is a dimer case of the sensitized luminescence experiment in crystals[32,33] which has been explained in detail elsewhere.[6] The monitored quantum yield or luminescence intensity contains information about the dynamics of the quasiparticle.

The probabilities $P_{1,2}(t)$ that the excitation resides on the two sites of the dimer obey

$$\frac{dP_1(t)}{dt}+\frac{P_1}{\tau}=\int_0^t ds\mathscr{W}'(t-s)[P_2(s)-P_1(s)], \tag{4.1}$$

$$\frac{dP_2(t)}{dt}+\frac{P_2}{\tau}+\Gamma P_2=\int_0^t ds\mathscr{W}'(t-s)[P_1(s)-P_2(s)], \tag{4.2}$$

$$\frac{dP_\theta(t)}{dt}+\frac{P_\theta}{\tau}=\Gamma P_2, \tag{4.3}$$

where $P_\theta(t)$ denotes the probability of occupation at the trap which extracts the excitation from site 2 at rate Γ, and τ is the radiative lifetime. As shown elsewhere,[33] the quantity $\mathscr{W}'(t)$ appearing in (4.1) and (4.2) equals the product of the memory $\mathscr{W}(t)$ and the factor $e^{-t/\tau}$.

We denote the Laplace variable by ϵ, and use tildes to represent the Laplace transforms. The quantum yield of luminescence, defined as the ratio of the number of photons emerging radiatively from the trap to the number of photons put into the dimer, is

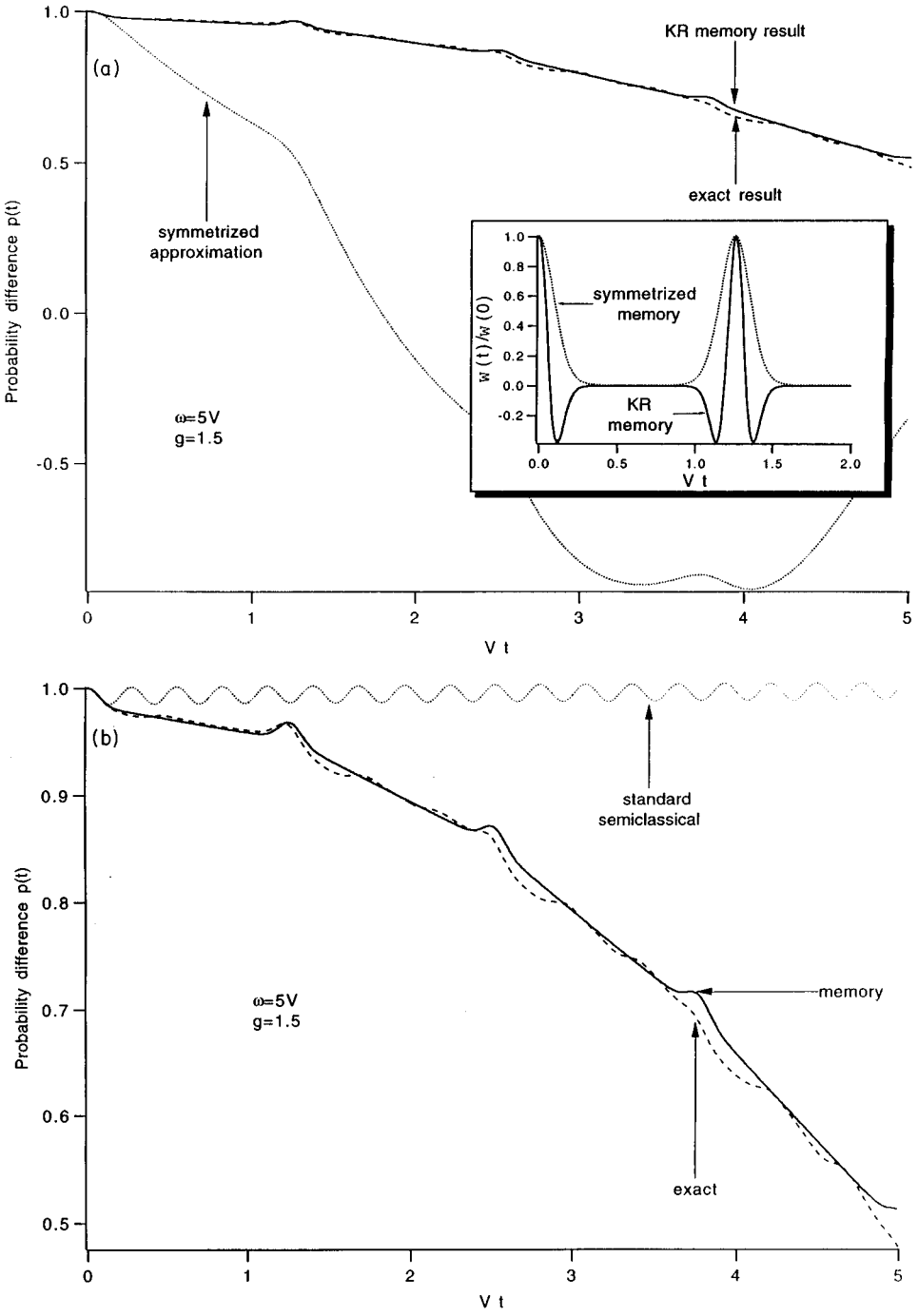

FIG. 3. Comparison of the memory function results to those of two semiclassical approximations. In (a), the symmetrized memory approximation (see text) is compared to the memory-function result and the exact result for parameter values $\omega=5V$, $g=1.5$. For the same parameter values, (b) shows the exact and memory results, respectively, compared to the standard semiclassical approximation. Both semiclassical approximations are found to be quite poor for the parameters chosen.

$$\phi=\frac{1}{\tau}\tilde{P}_{\theta}(0) \tag{4.4}$$

and is given explicitly by

$$\phi=\Gamma\tilde{P}_2(0)=\frac{\Gamma\tau\tilde{\mathscr{W}}(1/\tau)}{(1+\Gamma\tau)+\tau\tilde{\mathscr{W}}(1/\tau)(2+\Gamma\tau)}. \tag{4.5}$$

Since our interest is in examining the effect of the quasiparticle motion within the dimer on the yield observable, we take the limit of infinite Γ, which is appropriate to some realistic systems. The limit makes the trap parameter Γ disappear from the yield expression and allows us to concentrate on the effects of motion alone:

$$\phi=\frac{\tau\tilde{\mathscr{W}}(1/\tau)}{1+\tau\tilde{\mathscr{W}}(1/\tau)} \tag{4.6}$$

The observable ϕ is directly related to $\tilde{\mathscr{W}}(1/\tau)$, the key quantity in our memory approach. The yield is sensitive to different features of the motion according to which time scale of the memory function is comparable to the experimental probe time τ. The quantum yield probe is thus particularly appropriate in the context of our memory approach. For comparison, the memory $\tilde{\mathscr{W}}(\epsilon)$ corresponding to *any* calculational approach, e.g., the exact or the semiclassical method, can be obtained from the probability difference $p(\tilde{\epsilon})$ through

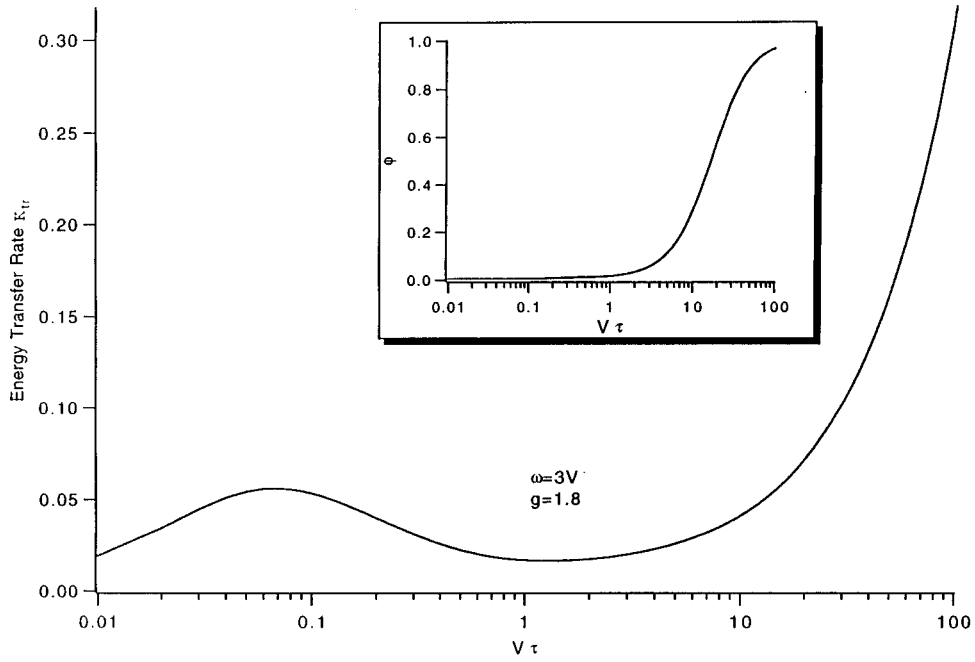

FIG. 4. The energy-transfer rate $\mathscr{K}_{\rm tr}$ for sensitized luminescence is plotted logarithmically against $V\tau$ for the parameters of Fig. 2: $g=1.8$, $\omega=3V$, calculated with the memory approach on ω. The inset shows the quantum yield ϕ.

$$2\tilde{\mathscr{W}}(\epsilon)=\frac{1}{p(\tilde{\epsilon})}-\epsilon. \tag{4.7}$$

The overall features of the yield in (4.6), as $V\tau$ changes, are a rise and saturation to 1. Closely related to the quantum yield is the energy-transfer rate,[6,32,33]

$$\mathscr{K}_{\rm tr}=\frac{1}{\tau}\frac{\phi_G}{\phi_H}=\frac{1}{\tau}\frac{\phi}{1-\phi}, \tag{4.8}$$

which exhibits more detailed features of the motion. In (4.8) the subscript G refers to the guest (or trap) site and the subscript H refers to the host sites. The last equality in (4.8) follows from the assumption that the radiative decay rates are the same for the hosts and the guests. From (4.6) and (4.8), it is clear that the energy-transfer rate is identical to the Laplace transform of the memory function $\mathscr{W}(t)$ evaluated at $1/\tau$,

$$\mathscr{K}_{\rm tr}=\frac{1}{\tau}\frac{\phi}{1-\phi}=\tilde{\mathscr{W}}. \tag{4.9}$$

Figure 4 shows the energy-transfer rate $\mathscr{K}_{\rm tr}$ plotted logarithmically against $V\tau$. Shown in the inset is the corresponding behavior of the yield ϕ. The rapid rise in the transfer rate for small values of τ stems from the fact that, in the time domain, the memory function drops rapidly initially. In particu-

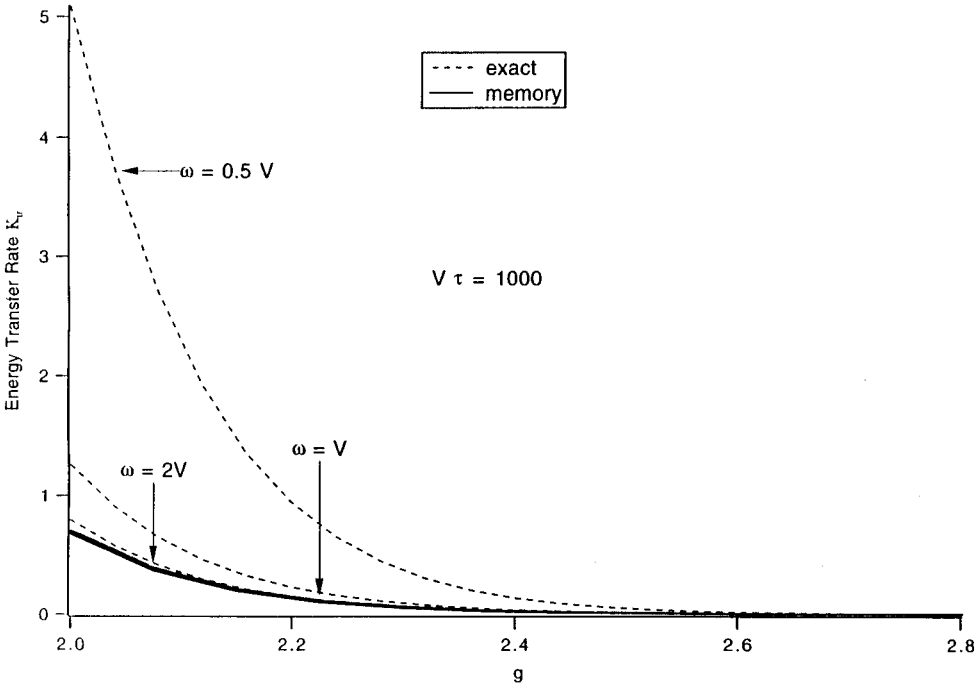

FIG. 5. Dependence of the energy-transfer rate $\mathscr{K}_{\rm tr}(\tau)$ on the coupling constant for various values of the oscillator frequency as calculated from the memory approach (solid line) and the exact calculation (dashed line). Note that, for the parameters chosen, the rates computed from the memory-function approach for $\omega=0.5V,V,2V$ all practically coincide.

lar, the peak of the energy-transfer rate occurs at $V\tau \approx 1/(2g^2\omega)$ which, in the massive oscillator limit, is the frequency of the rapid oscillations of the memory function. The slope of the energy-transfer rate for large values of $V\tau$ gives the average value of the memory function $\mathscr{W}(t)$ which is equal to $2V^2e^{-2g^2}$. If the radiative lifetime τ were a quantity under experimental control, the essential parameters of the system could thus be extracted from the dependence of the yield observable on the lifetime. Unfortunately, in real systems, τ cannot be varied in this fashion. The purpose of the above analysis is largely illustrative and the role of τ should be regarded as that of a time probe.

The variation of $\mathscr{K}_{\rm tr}$ seen in Fig. 4 can be understood very simply by realizing that the memory function $\mathscr{W}(t)$ behaves in its gross characteristics as the sum of a constant and a repeated damped exponential:

$$\mathscr{W}(t) \approx f(t) = 2V^2 \sum_{n=0}^{\infty} e^{-\alpha(t-2n\pi/\omega)} \cos(\Omega t)\,\theta(t-2n\pi/\omega) + 2V^2 e^{-2g^2}, \tag{4.10}$$

where $\theta(t)$ is the Heaviside step function. For large values of g and small values of ω, the illustrative parameters of $f(t)$, viz., α and Ω, are, respectively, of the order of $g\omega$ and $g^2\omega$. The Laplace transform of $f(t)$ can be trivially calculated:

$$\tilde{f}(1/\tau) = 2V^2 \left(\frac{\alpha_1\{1-e^{-\alpha_1/\varpi}\cos(\Omega/\varpi)\} + \Omega e^{-\alpha_1/\varpi}\sin(\Omega/\varpi)}{[1-\exp(-1/\varpi\tau)][\alpha_1^2+\Omega^2]} + e^{-2g^2}\tau \right), \tag{4.11}$$

where $\varpi = \omega/2\pi$, $\alpha_1 = \alpha + 1/\tau$. The transform possesses the essential feature of $\mathscr{K}_{\rm tr}$, viz., an initial rise followed by a drop to zero, and an eventual linear increase for large values of $V\tau$.

The energy-transfer rate as predicted by the memory function is particularly sensitive to g and almost completely insensitive to ω for the parameters shown in Fig. 5, which displays the dependence of the energy-transfer rate on g for various values of ω. We show both the memory results (solid line) and the consequences of the exact evolution (dashed line), the latter obtained through the use of (4.7). One notices that the transfer rate drops sharply as one changes the value of g from 2 to 3, for a range of values of ω. One also notices that the memory function appearing in (2.14) predicts an energy-transfer rate that approaches the true energy-transfer rate coming from the exact evolution as one increases g but differs from the true energy-transfer rate for small g. The agreement also improves as one increases ω/V. Both these trends are in keeping with the expectation that the memory-function treatment improves in accuracy as the ratio $g^2\omega/V$ increases. The value of $V\tau$ that we have chosen here corresponds to a normal experimental system in which V and τ are of the order of a few wave numbers and a few nanoseconds, respectively. The independence of the memory function result on ω seen in Fig. 5 is not a general consequence for arbitrary parameters.

V. THREE PHYSICAL SYSTEMS

In this section, we present an examination of three physical systems with the help of the memory-function formalism and the semiclassical approximation. The experimental observables are charge mobility in aromatic hydrocarbons, thermal diffusivity in high-temperature thermoelectrics, and vibrational energy transfer in biological systems like proteins.

The first of the three phenomena involves observations of the mobility of photoinjected charge carriers in naphthalene. The moving quasiparticle is generally a hole or an electron, and it interacts strongly with librational phonons of the lattice.[3] Values of the system parameters have been extracted earlier.[3] The coupling constant is $g=1.8$, the carrier bandwidth is 10.5 meV, and the librational phonon energy is 16 meV. From these we find that, in the notation of the present paper, $g=1.8$, $V=60$ K, and $\omega/V=3.2$. Within this section, we write $\hbar$ explicitly to facilitate comparison with experimental values. Although the dimer studied in the present paper cannot completely represent a crystal, we will assume, as a working hypothesis (for simplicity), that the essential physics behind the effects of strong interaction between a quasiparticle and phonons is captured by this comparison to the dimer. This assumption will be made for all the three systems studied in this section. Figure 6(a) shows a comparison of the results due to the exact quantum-mechanical calculation, semiclassical approximation, and memory-function analysis. It is clear that, whereas the semiclassical approximation fails quite badly, the memory function recovers all the salient features of the exact evolution. In particular, the short-time evolution at a frequency of $g^2\omega$, the decay of the initial oscillations at a time of $1/g\omega$, the revival of the oscillations at a frequency of ω, and the tunneling to the other site at a time of approximately $1/e^{-g^2}$ are all shown by the memory analysis.

The second phenomenon we analyze is anomalous thermal conduction observed in boron carbides at high temperatures.[34,35] One of the observed features is that, while in B_4C thermal diffusivity displays ''normal'' behavior in that it decreases with increasing temperature, in B_9C it is nearly temperature independent. This feature was addressed in Ref. 35 by assuming the heat current to be due to carrier phonons whose frequency is modulated by lower-frequency phonons that ''dress'' the carrier phonons through strong interactions. One finds[35] that the ratio between the intersite matrix element to the phonon energy V/ω_D is 0.06, the coupling constant g is 0.6, and the phonon energy $\hbar\omega_D = k_B T_D = 1300$ K. In the above, the subscript D refers to the fact that the frequency of the dressing phonons has been taken to be the Debye frequency. In the notation of the present paper, the system parameters are $g=0.6$, $V=83.2$ K,

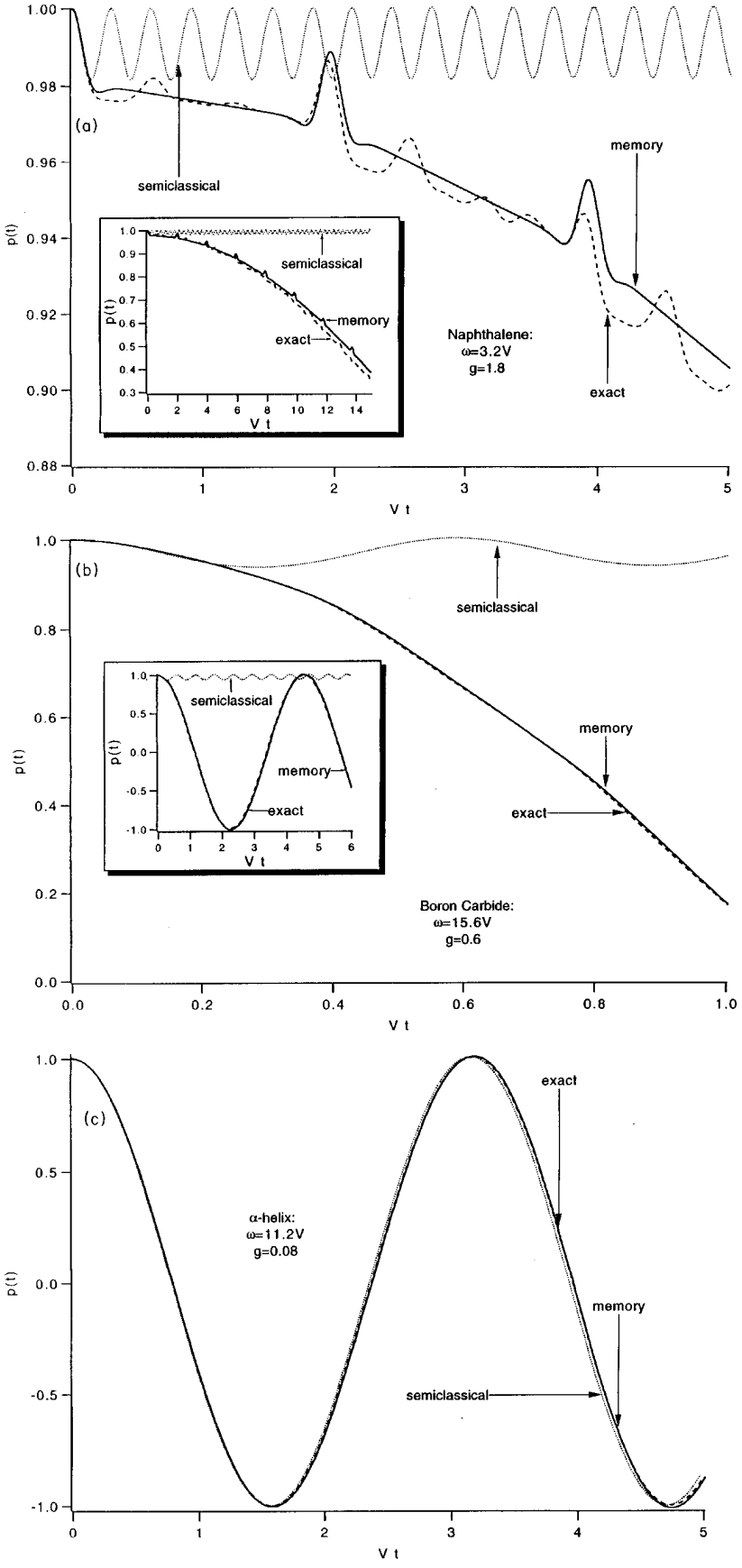

FIG. 6. Evolution in three physically relevant systems: (a) charge carrier transport in aromatic hydrocarbon crystals, (b) thermal diffusion in high-temperature thermoelectrics, and (c) vibrational energy transfer in biological systems. Exact (dashed line), memory (solid line), and semiclassical (dotted line) results for the evolution of the quasiparticle probability in a representative two-site system are compared. All three curves in (c) are almost identical to one another and are practically indistinguishable from the result for zero interaction between the quasiparticle and vibrations.

and $\omega/V=15.6$. Figure 6(b) shows a comparison between the numerically exact calculation (dashed line), the memory-function result (solid line), and the semiclassical result (dotted line). The first two are in agreement whereas the semiclassical approximation departs from both very early. In particular, since $g<1$, the quasiparticle tunnels out quickly. The semiclassical approximation fails to capture this feature, and erroneously predicts self-trapping.

The third system we address is the Davydov soliton[36] which provides a mechanism for the localization and transport of vibrational energy in protein. In this mechanism, vibrational energy of the CO stretching (or Amide-I) oscillators localized on the α-helix region of the protein is supposed, through a phonon coupling effect, to act to distort the helix structure. The helical distortion reacts, also through phonon coupling, to prevent Amide-I oscillation energy dispersion, causing self-localization. The parameters involved in this field have been a subject of some debate. We take those given in the review of Scott[13] who describes a model involving longitudinal compression waves and one representative mode of vibration. The Hamiltonian is

$$\hat{H}=\hat{H}_{\rm ex}+\hat{H}_{\rm ph}+\hat{H}_{\rm int}, \tag{5.1a}$$

$$\hat{H}_{\rm ex}=\sum_n E_0 B_n^\dagger B_n - J(B_n^\dagger B_{n+1}+B_n^\dagger B_{n-1}), \tag{5.1b}$$

$$\hat{H}_{\rm ph}=\frac{1}{2}\sum_n \left(\frac{\hat{p}_n^2}{\tilde{M}}+\tilde{w}(\hat{u}_{n+1}-\hat{u}_n)^2\right), \tag{5.1c}$$

$$\hat{H}_{\rm int}=\chi\sum_n (\hat{u}_{n+1}-\hat{u}_n)B_n^\dagger B_n . \tag{5.1d}$$

The coupling parameter χ has been estimated to be 35 pN (Ref. 13) and 62 pN.[37] The symbol χ in this section has been reserved for the quasiparticle-phonon coupling parameter in conformity with Ref. 13 and should not be confused with the polaron binding energy χ $(2g^2\omega)$ mentioned elsewhere in this paper. The longitudinal spring constant $\tilde{\omega}$ is three times that for a single hydrogen bond, which in turn, is estimated from experiments to be 13 N/m (Ref. 38), and from *ab initio* calculations to be 19.5 N/m.[13] The mass $\tilde{M}$ of the lattice oscillator is three times the average mass of an amino acid molecule in myosin,[39] which in turn is 1.9×10^{-25} kg. The transfer interaction J has been calculated from electromagnetic theory[40] to be 1.55×10^{-22} J. The interaction term in (5.1c) $\hat{H}_{\rm int}$ is given by

$$\hat{u}_n=\sum_q \left(\frac{\hbar}{2N\tilde{M}\omega_q}\right)^{1/2} e^{iqnl}(b_q+b_{-q}^\dagger), \tag{5.2}$$

where l is the lattice spacing (the distance between peptide groups) and the frequency ω_q of the oscillator is given by the dispersion relation $\omega_q=2(\tilde{\omega}/\tilde{M})|\sin(ql/2)|$. In the notation of the present paper, the phonon frequency ω thus varies between 1.6×10^{13} and 2.0×10^{13} rad/s, the intersite matrix element V is 11.2 K, and the quasiparticle-phonon coupling energy $\hbar g\omega=\chi\sqrt{\hbar/2\tilde{M}\omega_q}$ varies between 0.75×10^{-22} and 1.5×10^{-22} J. Thus, g varies between 0.035 to 0.084, and the ratio of the phonon energy to the intersite matrix element $\hbar\omega/V$ varies between 11.2 and 13.8. Figure 6(c) shows a comparison between the exact result, the memory-function prediction, and the semiclassical approximation result, all of which show free (not self-trapped) evolution, and agree with one another. Close inspection of the values obtained reveals two features: (i) the memory approach is slightly better in representing the exact evolution than the semiclassical approximation but the difference is not significant, (ii) all three curves are hardly distinguishable from the plot $p(t)=\cos(2Vt)$ characteristic of evolution in which the quasiparticle-vibration interaction *is zero*.

TABLE I. Parameters of the three systems.

System	g	$\hbar\omega/V$	$\hbar g\omega/V$	$\hbar g^2\omega/V$
Naphthalene	1.8	3.2	5.9	10.7
Boron carbide	0.6	15.6	9.4	5.6
α-helix	0.035–0.084	11.2–13.8	0.48–0.94	0.017–0.079

We see that in all three cases considered above, the memory-function approach fares rather well in representing the actual evolution. The semiclassical approach does poorly in two of the three cases. In the third, i.e., vibrational transfer in protein, where it represents the exact evolution well, the interaction with vibrations is too small to have *any* effect on the quasiparticle evolution. We certainly cannot claim to have established the shortcomings of the semiclassical approach for any of these physical systems since the actual systems are extended crystals or aggregates in interaction with a large number of modes. Our model, by contrast, is merely a dimer in interaction with a single mode. It is not inconceivable that the introduction of the additional degrees of freedom will change some of the quantitative conclusions. However, within the confines of the simplified model, the indication is unmistakable: the semiclassical approach tends to be inadequate or of little use, while the memory approach approximates the exact evolution satisfactorily. We summarize the parameters of the three systems in Table I.

VI. DISCUSSION

We have seen that the memory-function approach introduced many years ago for charge and excitation transport[6,11,12] provides an excellent approximation to the exact evolution of the standard quasiparticle-phonon system (2.1) underlying many recent polaron, exciton, and quantum soliton discussions, at least for the single-mode zero-temperature dimer system analyzed in this paper. An examination of its validity for many modes, arbitrary temperature, and extended systems is important but difficult to undertake. Work along those lines is in progress. The starting point for our memory approach is generally (2.10), which is an exact consequence of the dynamics, and specifically (2.14), which is the result of the initial condition we assume and the perturbation scheme we employ for the analysis of the single-mode zero-temperature dimer of (2.2). We have seen that the memory approach is able to describe adequately a number of features carrying the signature of the exact evolution. An additional advantage of the approach is that the source of the features is made transparent. The quantum yield experiment that we have described in Sec. IV is particularly amenable to analysis through the memory approach.

The memory approach,[6,11,12] specifically the evolution equation (2.14), appears to be closely related (for all practical purposes identical) to the more recent noninteracting blip approximation (NBA) treatment[41] given on the basis of a quite different and considerably more complex formalism. The work of Grigolini and co-workers[19,20] has made it clear that their approach, in one of its simplified forms, is equiva-

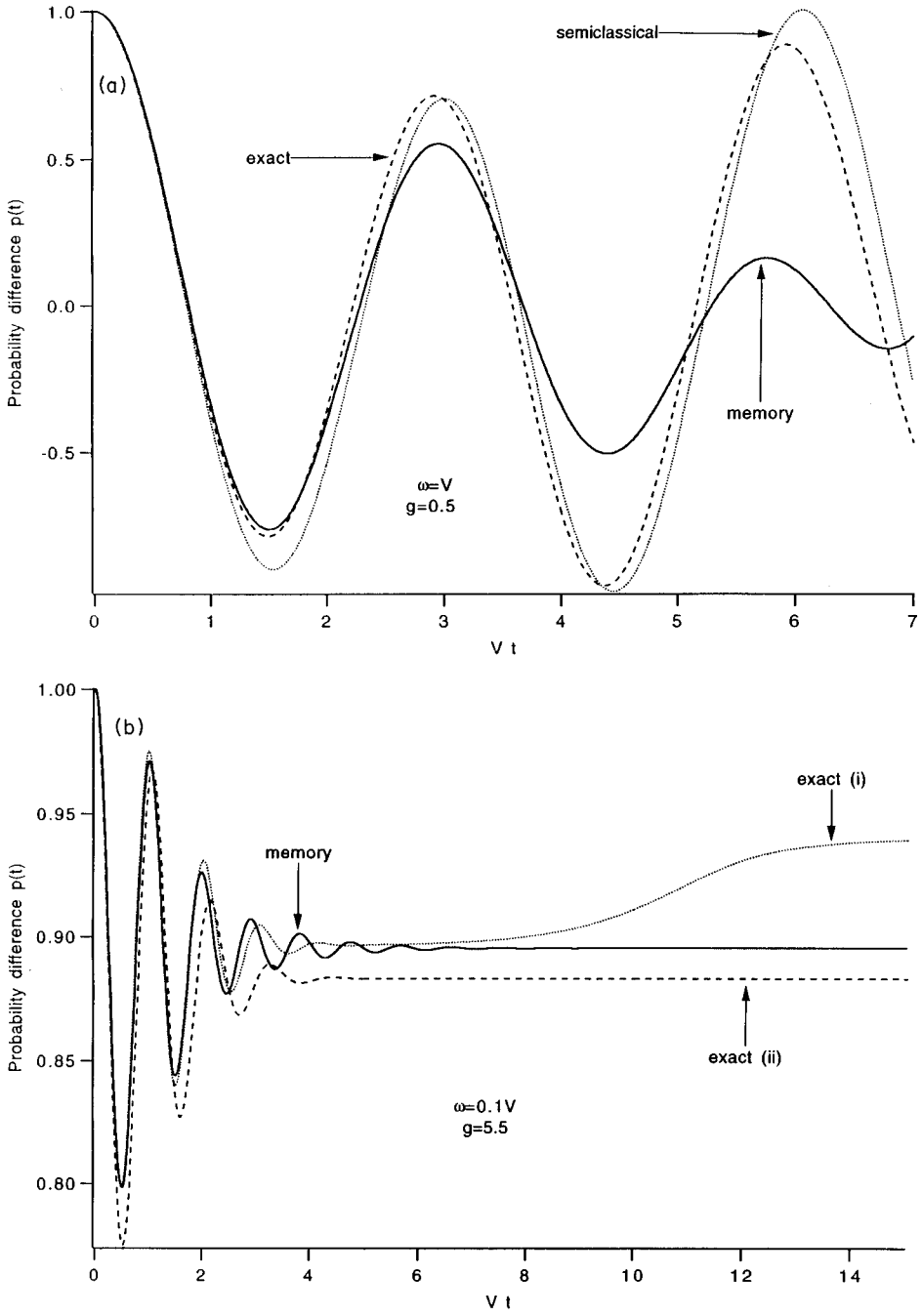

FIG. 7. Breakdown of the memory-function approach. (a) Comparison between the exact result, the semiclassical approximation, and the memory-function approach in a regime where the semiclassical approach is better than the memory approach. The parameters are $\omega=V$, $g=0.5$. (b) Comparison of the memory result with exact results for two different initial conditions. The initial state for the memory result is the same as that for the exact result (i) but different from that for (ii). See text. The parameters are $\omega=0.1V$, $g=5.5$ as in Fig. 1(c) of Ref. 22.

lent to the NBA analysis. It is easy to appreciate that the simplified equation used by Grigolini and co-workers to analyze the dimer[19,20] is a short-time expansion of our memory equation (2.14). It is remarkable that this connection between the memory approach[6,11,12] and the noninteracting blip approximation[41] has remained undiscovered for so long. Given the considerable ease of derivation involved in the memory method, and the great deal of interest that the NBA has stimulated in the literature, it seems likely that useful insights into the general problem of quasiparticle-boson interaction will be gained with the help of this connection.

The essential components of the memory approach are the use of projections to concentrate on the quasiparticle dynamics by tracing over the phonons, a perturbation expansion in orders of the transfer interaction after the dressing transformation, and the use of a certain class of initial conditions. In the form presented here, attention has also been focused on the evolution of the quasiparticle probabilities, thus making it easy to obtain $p(t)$ and $q(t)$ but not $r(t)$ directly. This is easily remedied by excluding the diagonalizing feature of the projection operators as might be done to obtain the so-called stochastic Liouville equation,[4,5,10] i.e., a density matrix equation (rather than a probability equation) for the quasiparticle. Further work requires to be done on the memory approach in two important directions: (i) study of the precise domain of the validity of the approach, (ii) the initial condition problem. We comment on each in turn.

The Hamiltonian of (2.2) [generally of (2.1)] is characterized by three energies: the transfer interaction V, the oscillator energy ω, and the interaction energy $g\omega$. When we focus attention on quasiparticle dynamics (rather than phonon dynamics), we see that two of the phenomena, viz., transfer and

interaction with phonons, compete for domination of the evolution. The problem can be solved analytically in the two limits $g \to 0$ and $V \to 0$, the respective characteristic energies of the quasiparticle being V and $g^2\omega$. It is important to notice that the latter is not $g\omega$. The perturbation parameter whose smallness may be said to mark the validity domain of the memory approach is $V/g^2\omega$. If this parameter is not too small, it is possible (but tedious) to develop memory functions which involve higher terms in the perturbation expansion. In order to show a regime in which the memory approach does not do as well as the semiclassical approximation, we choose $g < 1$ and ω comparable to V. This allows us to approximate the massive oscillator limit which validates the semiclassical approximation and at the same time violate the perturbation scheme based on $V \leqslant g^2\omega$. Figure 7(a) shows a comparison between $p(t)$ as predicted by the exact result (dashed line), by the memory-function approach (solid line) and the semiclassical approximation (dotted line) for such a case: $\omega = V$, $g = 0.5$. The initial condition used is that the quasiparticle is localized on one site, and the phonons are in the ground state of the displaced oscillator basis. In this weak-coupling, intermediate phonon frequency ($\omega \approx V$) regime, we see that, as expected, the semiclassical approximation is better than the memory-function approximation. This regime does *not* correspond to polaron formation, however. (Note that $g < 1$.) The advantage of employing the semiclassical approximation over the memory-function approach appears thus to be limited to nonpolaronic and relatively uninteresting regimes. It is interesting that the memory approach for the dimer provides a good approximation for *both* large g and small g. The first of these results is easily understandable since the perturbation parameter $V/g^2\omega$ is small. In the opposite (weak-coupling) limit $g \to 0$, the memory function tends to the constant value $2V^2$ which corresponds to the exact evolution in the absence of quasiparticle-vibration coupling. This fact, that the memory function becomes trivially exact in the limit of vanishing g, is indicated in Fig. 6(c).

We now turn to the initial condition term. The derivation of (2.14), in the more general form of Refs. 11 and 12 requires that the initial phonon state be thermal in the unperturbed transformed Hamiltonian eigenstates. For the zero-T single-mode case, this means that the initial phonon state is the ground state of the displaced oscillator basis. The exact numerical solutions we have shown here so far, with the exception of Fig. 7(a), are based on the assumption that the initial state is a one-site projection of the ground state of the *total* Hamiltonian. These two initial states are identical to each other for large g's. However, for small g's, they can differ considerably. The corresponding time evolutions also differ, as Fig. 7(b) shows. The validity of the assumption involved in this replacement of the actual initial state by the approximate counterpart has to be investigated. Work is in progress on an extension of the memory approach to arbitrary initial conditions through a modification of the projection operator.

In summary, our present study supports the conclusions drawn by Grigolini and co-workers[18–20] that semiclassical equations of motion for the Hamiltonian of (2.1) could be questionable in many physically relevant cases. It agrees with the recent analysis[18–20] as well as early concerns[21] that had been raised regarding the semiclassical approximation. Our study also goes further in showing a clear limit in which the semiclassical approximation is valid, and in suggesting a simple and well-tested alternative for approximate analysis: Our memory approach[6,11,12] should complement other methods put forward recently such as the Wigner-distribution method.[18]

[1] R. Silbey and R. W. Munn, J. Chem. Phys. **72**, 2763 (1980); see also R. Silbey, Ann. Rev. Phys. Chem. **27**, 203 (1976).

[2] L. B. Schein, C. B. Duke, and A. R. McGhie, Phys. Rev. Lett. **40**, 197 (1978); C. B. Duke and L. B. Schein, Phys. Today **33** (2), 42 (1980).

[3] V. M. Kenkre, J. D. Andersen, D. H. Dunlap, and C. B. Duke, Phys. Rev. Lett. **62**, 1165 (1989); V. M. Kenkre and D. H. Dunlap, Philos. Mag. **65**, 831 (1992).

[4] M. Grover and R. Silbey, J. Chem. Phys. **53**, 2099 (1970); **54**, 4843 (1971).

[5] H. Haken and P. Reineker, Z. Phys. **249**, 253 (1972).

[6] V. M. Kenkre, in *Exciton Dynamics in Molecular Crystals and Aggregates*, edited by G. Höhler (Springer, Berlin, 1982), p. 1.

[7] *Hydrogen in Metals*, edited by G. Alefeld and J. Völkl (Springer, New York, 1978), Vol. 1.

[8] *Muon Spin Rotation*, edited by J. H. Brewer and P. W. Percival (North-Holland, Amsterdam, 1981).

[9] L. D. Landau and S. Pekar, Zh. Eksp. Teor. Fiz. **16**, 341 (1942); T. D. Holstein, Ann. Phys. **8**, 343 (1959).

[10] P. Reineker, in *Exciton Dynamics in Molecular Crystals and Aggregates* (Ref. 6), p. 111.

[11] V. M. Kenkre and T. Rahman, Phys. Lett. A **50**, 170 (1974).

[12] V. M. Kenkre, Phys. Rev. B **12**, 2150 (1975).

[13] A. C. Scott, Phys. Rep. **217**, 1 (1992); see, also, *Davydov's Soliton Revisited: Self-Trapping of Vibrational Energy in Protein*, edited by P. L. Christiansen and A. C. Scott (Plenum, New York, 1990).

[14] J. C. Eilbeck, A. C. Scott, and P. S. Lomdahl, Chem. Phys. Lett. **113**, 29 (1985); Physica **16D**, 318 (1985).

[15] V. M. Kenkre and D. Campbell, Phys. Rev. B **34**, 4959 (1986); V. M. Kenkre, in *Singular Behaviour and Nonlinear Dynamics*, edited by St. Pnevmatikos, T. Bountis, and Sp. Pnevmatikos (World Scientific, Singapore, 1989).

[16] V. M. Kenkre, Physica D **68**, 153 (1993).

[17] See, e.g., V. M. Kenkre and L. Cruzeiro-Hansson, Z. Phys. B **95**, 379 (1994); V. M. Kenkre, S. Raghavan, and L. Cruzeiro-Hansson, Phys. Rev. B **49**, 9511 (1994); L. Cruzeiro-Hansson and V. M. Kenkre, Phys. Lett. A **190**, 59 (1994).

[18] D. Vitali, P. Allegrini, and P. Grigolini, Chem. Phys. **180**, 297 (1994).

[19] L. Bonci, P. Grigolini, and D. Vitali, Phys. Rev. A **42**, 4452 (1990).

[20] L. Bonci, P. Grigolini, R. Roncaglia, and D. Vitali, Phys. Rev. A **47**, 3538 (1993); L. Bonci, R. Roncaglia, B. J. West, and P. Grigolini, *ibid*. **45**, 8490 (1992); D. Vitali and P. Grigolini, *ibid*. **42**, 7091 (1990); P. Grigolini, Int. J. Mod. Phys. B **6**, 171 (1992).

[21] See, also, early objections to the semiclassical treatment given by D. Brown, B. West, and K. Lindenberg, Phys. Rev. A **33**, 4110 (1986); D. Brown, K. Lindenberg, and B. West, Phys. Rev. B **35**, 6169 (1987); and by W. C. Kerr and P. S. Lomdahl, *ibid*. **35**, 3629 (1987).

[22] M. Salkola, A. R. Bishop, V. M. Kenkre, and S. Raghavan, Phys. Rev. B **52**, R3824 (1995).

[23] Consistency of notation in the literature, while desirable, is generally impossible. The notation followed below is as in Refs. 16 and 17. Some of its relations to the notation in Ref. 22 are g, $\hat{p}$, $\hat{q}$, $\hat{r}$, $\hat{y}$, and $\hat{\pi}_y$ in the present paper correspond to λ/ϵ_0, $\hat{\sigma}_3$, $\hat{\sigma}_2$, $\hat{\sigma}_1$, $\hat{\phi}$, and $\hat{\pi}$, respectively, in Ref. 22.

[24] T. D. Lee, F. E. Low, and D. Pines, Phys. Rev. **90**, 297 (1953); see also H. Haken, *Quantum Field Theory of Solids: An Introduction* (North-Holland, Amsterdam, 1976).

[25] I. G. Lang and Y. A. Firsov, Zh. Eksp. Teor. Fiz. **43**, 1843 (1962) [Sov. Phys. JETP **16**, 1301 (1963)].

[26] For spatially extended systems, it is customary (and necessary) to neglect the term proportional to $\hat{P}^2$ as in Refs. 1, 4, 6, and 12.

[27] R. W. Zwanzig, in *Lectures in Theoretical Physics*, edited by W. Downs and J. Downs (Boulder, Colorado 1961), Vol. III; in *Quantum Statistical Mechanics*, edited by P. H. E. Meijer (Gordon and Breach, New York, 1966).

[28] V. M. Kenkre and M. Dresden, Phys. Rev. Lett. **27**, 9 (1971).

[29] D. Brown, K. Lindenberg, and B. West, Phys. Rev. A **37**, 2946 (1988); see, in particular, the Appendix.

[30] R. Kubo, J. Phys. Soc. Jpn. **12**, 570 (1957).

[31] L. van Hove, Physica **21**, 517 (1955); also, in *Fundamental Problems in Statistical Mechanics*, edited by E. G. D. Cohen (North-Holland, Amsterdam, 1962).

[32] H. C. Wolf, in *Advances in Atomic and Molecular Physics*, edited by D. R. Bates and I. Estermann (Academic, New York, 1967), Vol. 3, p. 119; H. Auweter, U. Mayer, and D. Schmid, Z. Naturforsch. Teil A **33**, 651 (1978).

[33] V. M. Kenkre and Y. M. Wong, Phys. Rev. B **23**, 3748 (1981); V. M. Kenkre and D. Schmid, *ibid*. **31**, 2430 (1985); see, in particular, the appendix to this paper.

[34] C. Wood, D. Emin, and P. E. Gray, Phys. Rev. B **31**, 6811 (1985).

[35] V. M. Kenkre and X. Fan, in *Novel Refractory Semiconductors*, edited by D. Emin, T. L. Aselage, and C. Wood, MRS Symposia Proceedings No. 97 (Materials Research Society, Pittsburgh, 1987), p. 89. See, also, X. Fan, Ph.D. thesis, University of New Mexico, 1990.

[36] A. S. Davydov, J. Theor. Biol. **66**, 379 (1977).

[37] G. Careri, U. Buontempo, F. Galluzzi, A. C. Scott, E. Gratton, and E. Shyamsunder, Phys. Rev. B **30**, 4699 (1984).

[38] K. Itoh and T. Shimanouchi, J. Mol. Spectrosc. **42**, 86 (1972).

[39] A. C. Scott, Phys. Rev. A **26**, 578 (1982); **27**, 2767 (1983).

[40] Yu. N. Chirgadze and N. A. Nevskaya, Dokl. Akad. Nauk SSSR **208**, 447 (1973); N. A. Nevskaya and Yu. N. Chirgadze, Biopolymers **15**, 637 (1976); J. C. Eilbeck, P. S. Lomdahl, and A. C. Scott, Phys. Rev. B **30**, 4703 (1984).

[41] A. J. Leggett, S. Chakravarty, A. T. Dorsey, M. P. A. Fisher, A. Garg, and W. Zwerger, Rev. Mod. Phys. **59**, 1 (1987).